Channel Estimation on the Forward Link of Multi-beam Satellite Systems

Michael Bergmann[1], Wilfried Gappmair[1], Carlos Mosquera[2], and Otto Koudelka[1]

[1] Institute of Communication Networks and Satellite Communications
Graz University of Technology, Austria
{michael.bergmann,gappmair,koudelka}@tugraz.at
[2] Department of Signal Theory and Communications
University of Vigo, Spain
mosquera@gts.tsc.uvigo.es

Abstract. Multi-beam concepts are an essential component of next generation broadband satellite systems. Due to aggressive design goals, full frequency reuse is suggested in this context so that appropriate interference mitigation techniques have to be applied on both forward and return links. In this respect, channel estimation is of paramount importance. Throughout this paper, we are focusing on channel estimation of the forward link with emphasis on orthogonal and non-orthogonal training sequences used for this purpose. By analytical and simulation results, it is confirmed that the former are best suited in terms of the obtained jitter performance. On the other hand, non-orthogonal codes are not restricted by their length, but it is shown that a linearly independent set of unique words is significantly affected by an amplification of the noise component – a result not available from the technical literature on this subject so far. Furthermore, it is demonstrated that a simple correlation procedure, which might be employed for any kind of non-orthogonal training sequences, produces a non-negligible jitter floor in the higher SNR regime, which is primarily given by the cross-correlation properties of the code.

Keywords: Channel estimation, multi-beam satellite systems, forward link, orthogonal and non-orthogonal training sequences.

1 Introduction

Compared to terrestrial solutions, the major benefit of satellite communications is that all users can be served at the same cost factor within the coverage zone. In this context, it is well known that the potential of a single-beam system is limited in terms of availability and throughput – in contrast to an approach based on multiple or even full *frequency reuse* [1]. Therefore, with regard to next generation broadband satellite systems, it is suggested to consider a multi-beam technique, i.e., the coverage zone is served via a number of spot beams, suitably shaped by the antenna feeds forming part of the payload. Usually, the latter are controlled by a properly designed beamforming matrix [2]. In case the beam pattern must be modified, e.g., driven by the requirements of some mobile service, solely the matrix needs to be reorganized accordingly;

G. Giambene and C. Sacchi (Eds.): PSATS 2011, LNICST 71, pp. 250–259, 2011.

for reasons of flexibility and cost, it is intended in the near future to do that on ground [3].

Nevertheless, the multi-beam concept is closely related to a major problem: adjacent spots are heavily affected by *interference*, in particular if they employ the same frequency band. A fairly conservative answer for this sort of impairment is to employ a frequency reuse factor $f_R > 1$, i.e., adjacent user cells are served by different bands. There is no doubt that this decreases the spectral efficiency. As a consequence, upcoming satellite systems will be operated at full frequency reuse, i.e., $f_R = 1$, which means that all beams share the same spectrum, whereas the interference problem is to be mitigated by appropriately selected baseband algorithms. Most promising in this respect are linear or nonlinear precoding schemes on the forward link [4] and powerful interference cancellation techniques on the return link [5], [6].

Throughout this paper, we are focusing on the *forward link*, i.e., transmission of data from the centralized satellite gateway (GW) to the user terminals (UTs). Due to the fact that the GW controls the forward link (star topology), we assume a TDM-based (symbol-synchronous) concept. But no matter which kind of precoder we are going to implement at the end, for proper operation the corresponding channel estimates have to be known by the GW station. In this context, it makes sense to work with a data-aided approach [7], i.e., training sequences or unique words will be specified between GW and UTs. In the sequel, different solutions for channel estimation on the forward link will be investigated in detail by exploring the jitter variance as the most important figure of merit in this context.

The remainder of the paper is organized as follows. In Section 2, we introduce the signal model used for analytical and simulation work. Several channel estimators are discussed in Section 3, mainly by concentrating on the discrepancy between orthogonal and non-orthogonal training sequences. Numerical results are presented in Section 4, and conclusions are drawn in Section 5.

2 Signal Model

In the following, the forward link is considered to consist of an ideal satellite uplink (no fading or frequency-selective impacts) and an impaired downlink with full frequency reuse. It is assumed that the latter consists of $K = 100$ beams, pointing to 100 user cells, henceforth meant to serve 100 UTs simultaneously, i.e., a single UT per beam/cell at a given time. This is exemplified in Fig. 1 showing the 3 dB contour lines[1].

The 100 beams are formed by an antenna array with $N = 155$ feeds; each beam integrates 20 feeds tuned appropriately in amplitude and phase so as to achieve the required beamforming. Fig. 2 depicts a contour plot of the 155 feeds indicated by a separate number each; the contour lines represent the 3 dB attenuation limit of the respective feed. It is to be noticed that in our context channel estimation will be related to *feeds*, not beams, since it is supposed that interference mitigation techniques based on feeds will be more powerful [8], simply because $N >> K$, i.e., more degrees of freedom in the design of precoding and cancellation algorithms.

[1] This antenna model has been provided by the European Space Agency (ESA) in the framework of SatNEx-III for a study on next generation broadband satellite systems; such systems are primarily characterized by a multi-beam concept, data transmission in the Ka or even Q/V band, and the application of adaptive coding and modulation (ACM) strategies [11].

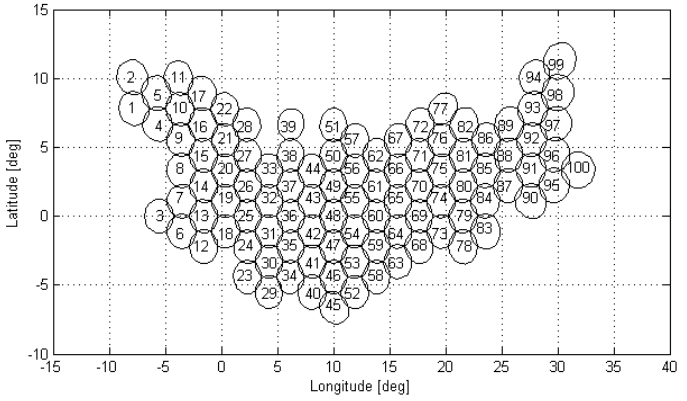

Fig. 1. Beam pattern (3 dB) generated by the satellite antenna

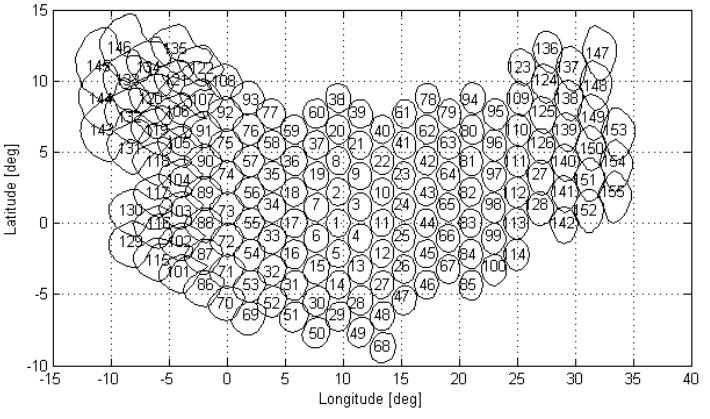

Fig. 2. Contour plot (3 dB) of the 155 satellite feeds

As already mentioned in the introductory section, a unique word (UW) is used to estimate the channel matrix **H** = **WGD**:

- **D** is the $N \times N$ matrix including transmitter GW effects, uplink, and on-board repeater chains; normally, **D** can be assumed as diagonal with the m-th entry representing the gain between feed m and GW station.
- **G** is the $K \times N$ feeder matrix; the entry (m, n) represents the gain between user link m and antenna feed n.
- **W** is the $K \times K$ diagonal fading matrix on the user downlink; the m-th entry represents the gain for user m.

In our signal model, the m-th line of **H**, i.e., $\mathbf{h}_m = (h_{m,1}, h_{m,2}, \ldots, h_{m,N})$, includes $N = 155$ complex-valued numbers characterizing the satellite downlink to the m-th UT, simply denoted by UT_m and as such sketched in Fig. 3. Considering this diagram, it is obvious that the estimation of each element in $\mathbf{h}_m$ suffers from a different

signal-to-noise ratio (SNR). For example, the signal power impinging from feed 119 at the UT_{48} (see Figs. 1 and 2) strongly differs from the signal power from feed 3, whereas noise power is the same for both; this has to be taken into account, when accuracy in terms of jitter variance is an issue throughout the estimation process.

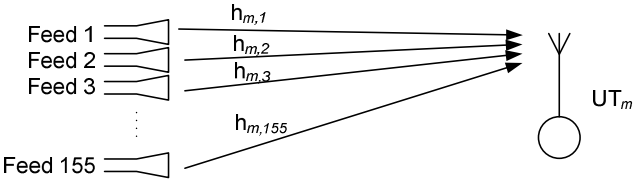

Fig. 3. Satellite downlink for the *m*-th user terminal

By inspection of Fig. 3, it is clear that the received signal at UT_m, i.e., $\mathbf{y}_m$ with $m = 1, 2, \ldots, K$, is given by

$$\mathbf{y}_m = \mathbf{h}_m \mathbf{C} + \mathbf{w}_m \tag{1}$$

where matrix $\mathbf{C}$ contains the complete set of $N = 155$ UWs as row vectors of length L and $\mathbf{w}_m$ denotes the sequence of zero-mean white Gaussian noise samples with variance $\sigma_w^2 = N_0/E_s$, where E_s/N_0 symbolizes the SNR per symbol.

3 Channel Estimation on the Forward Link

As already mentioned in the introductory section, the channel matrix $\mathbf{H}$ must be known to the GW station for interference mitigation on the forward link, e.g., realized by an appropriately selected precoding algorithm [9], [10]. This might be achieved by a separate calibration network; a more elegant and less expensive solution for this purpose, however, is the usage of the communication network as such. To this end, the estimates of $\mathbf{h}_m$, $m = 1, 2, \ldots, K$, will be collected by UT_m and reported to the GW via the return link.

The estimate of $\mathbf{h}_m$ is straightforwardly obtained by post-multiplying (1) with the Moore-Penrose pseudo-inverse of $\mathbf{C}$ expressed as $\mathbf{C}^+ = \mathbf{C}^H (\mathbf{C}\mathbf{C}^H)^{-1}$, where $\mathbf{C}^H$ denotes the Hermitean of $\mathbf{C}$. As a consequence, we arrive at

$$\hat{\mathbf{h}}_m = \mathbf{y}_m \mathbf{C}^+ = \mathbf{h}_m + \mathbf{e}_m \tag{2}$$

with the error vector evaluated as

$$\mathbf{e}_m = \mathbf{w}_m \mathbf{C}^+ . \tag{3}$$

3.1 Orthogonal UW Sequences

Orthogonal sequences are best suited for channel estimation since they do *not* produce interference noise. The reason is that the pseudo-inverse of $\mathbf{C}$ is in this case furnished

by the Hermitean transpose $\mathbf{C}^{\mathrm{H}}$, i.e., $\mathbf{C}\mathbf{C}^{\mathrm{H}} = \mathbf{I}$ so that (3) becomes $\mathbf{e}_m = \mathbf{w}_m \mathbf{C}^{\mathrm{H}}$. Having a closer look to $e_{m,i}$, which denotes the i-th entry of the error vector $\mathbf{e}_m$, we have that

$$e_{m,i} = \sum_{k=1}^{L} w_{m,k}\, c_{k,i}^{H} \tag{4}$$

where $c_{k,i}^{H}$ is the (k, i)-th element in $\mathbf{C}^{\mathrm{H}}$; normally, the codes are binary, i.e., the corresponding entries in $\mathbf{C}$ are given by $c_{k,i} = \pm 1$, so that $c_{k,i}^{H} = \pm 1/L$. In this respect, simply by taking into account that $E[|w_{m,k}|^2] = \sigma_w^2$, the total jitter variance for orthogonal sequences is straightforwardly derived as

$$\sigma_H^2 = \sigma_w^2 \sum_{i=1}^{L} |\, c_{k,i}^{H}\,|^2 = \frac{1}{L E_s / N_0}\,. \tag{5}$$

It is to be noticed that the frequently used Walsh-Hadamard codes are all of length $L = 2^n$, $n = 1, 2, 3, \ldots$ Therefore, randomly generated non-orthogonal sequences of arbitrary length L will be considered in the sequel.

3.2 Non-orthogonal UW Sequences

Basically, the pseudo-inverse $\mathbf{C}^{+}$ can be computed, if the UWs constituting matrix $\mathbf{C}$ are *linearly independent*. A necessary condition in this regard is that the length of the training sequence is equal or greater than the number of feeds, i.e., $L \geq N$. Then, according to (4), the i-th entry of the error vector $\mathbf{e}_m$ becomes

$$e_{m,i} = \sum_{k=1}^{L} w_{m,k}\, c_{k,i}^{+} \tag{6}$$

where $c_{k,i}^{+}$ is the (k, i)-th element in $\mathbf{C}^{+}$. Recalling again that the noise samples $w_{m,k}$ are zero-mean white Gaussian, the total jitter variance for linearly independent sequences is given by

$$\sigma_R^2 = \sigma_w^2 \sum_{k=1}^{L} |\, c_{k,i}^{+}\,|^2\,. \tag{7}$$

On the other hand, if $L < N$, the pseudo-inverse does *not* exist. In this case, we simply resort to a correlation procedure according to

$$\hat{\mathbf{h}}_m = \mathbf{y}_m \mathbf{C}^{H} \tag{8}$$

where the $N \times L$ matrix $\mathbf{C}$ necessarily includes some *linearly dependent* training sequences in form of row vectors. Moreover, it is to be observed that for linearly independent sequences, no matter if they are orthogonal or non-orthogonal, the jitter variance decreases with increasing values of $E_s/N_0 = 1/\sigma_w^2$, which is easily verified by inspection of (5) and (7). Confirmed by simulation results in the next section, this is in striking contrast to the correlation method producing a *jitter floor* for non-orthogonal codes, which is given by

$$\sigma_F^2 = \left| \sum_{m \neq k} \sum_{i=1}^{L} h_{m,i} c_{m,i} c_{k,i}^{*} \right|^2\,. \tag{9}$$

4 Numerical Results

Since $N = 155$ channels (feeder links) must be distinguished, Walsh-Hadamard (WH) codes require a length of $L = 2^8 = 256$ symbols in order to properly estimate the channel matrix **H**. Using this sort of UWs, Fig. 4 illustrates the simulation results for estimation accuracy in terms of the mean square error (MSE) for both magnitude (full dots) and angle of $h_{m,k}$ (open dots); with regard to the former, the values normalized by $|h_{m,k}|$ are shown and verified by the analytical relationship in (5): for higher E_s/N_0 values, the jitter variance for amplitude and phase of $h_{m,k}$ is given by $\sigma_H^2/2$ (solid line); note that the curve for phase estimates starts to flatten at $E_s/N_0 < -30$ dB, since they become more and more equally distributed between $\pm\pi$ so that the variance is given by $\pi^2/3$.

For a non-orthogonal code, based on randomly (RN) generated but linearly independent UWs with $L = 156$, Fig. 4 depicts the jitter performance of $h_{m,k}$ estimated at UT_{48} according to the scenario presented in Figs. 1 and 2. It can be seen that, in contrast to the ideal case (dashed line) indicating an assumed orthogonal code (OC) with $L = 156$, both angle and magnitude exhibit a significant degradation of the jitter variance given by $\sigma_R^2/2$ (dashed-dotted line, simulation results for magnitude/phase visualized by solid/open triangles). This is explained by the fact that, compared to WH sequences, the estimation procedure via RN schemes causes a non-negligible amount of additional noise introduced by $\mathbf{C}^+$ – to the best of the authors' knowledge, a result not discussed so far in the open literature. Finally, for $E_s/N_0 = 40$ dB, Fig. 5 shows the top view of the jitter performance as a function of the geographical location within the coverage zone (for normalization purposes, the strongest component of $\mathbf{h}_m$ is employed).

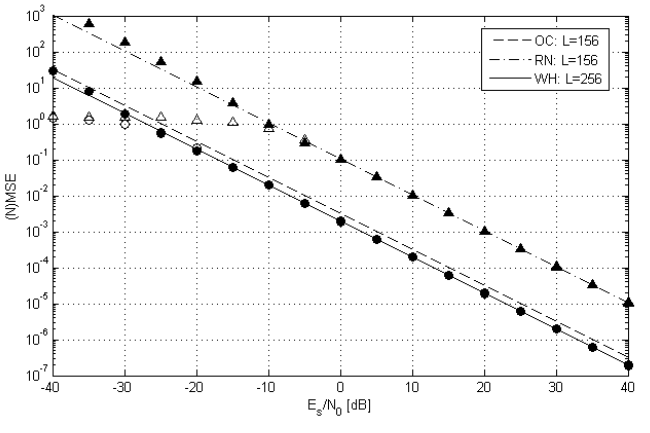

Fig. 4. Estimation accuracy for orthogonal and non-orthogonal codes achieved by the pseudo-inverse

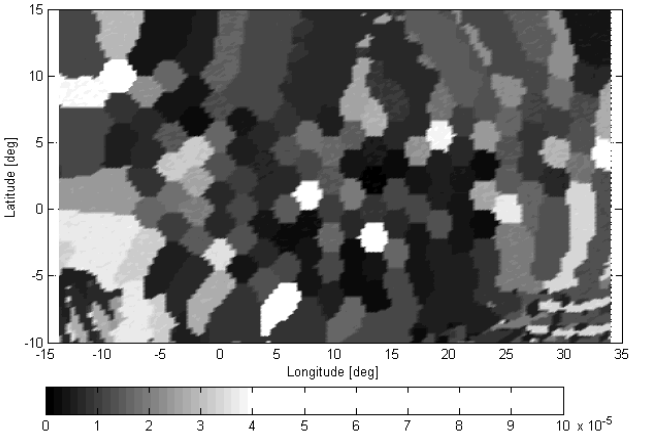

Fig. 5. Top view of estimation accuracy for non-orthogonal codes achieved by the pseudo-inverse (E_s/N_0 = 40 dB, L = 156)

For UT_{48} operated at L = 78, Fig. 6 shows the estimation accuracy using a set of RN sequences; but in contrast to the former case with L = 156, the UWs are now linearly dependent so that a pseudo-inverse does not exist. It can be seen that in the low SNR range, both the MSE of the angle (open dots/triangles) and the normalized MSE of the amplitude (full dots/triangles) are close to the theoretical limit $\sigma_H^2/2$ symbolizing an assumed orthogonal scheme (dashed/dashed-dotted line). Unfortunately, the estimation performance of the amplitude suffers from a significant jitter floor according to (9) in the higher SNR regime as can be observed by inspection of Fig. 6 (horizontal dashed/dashed-dotted line).

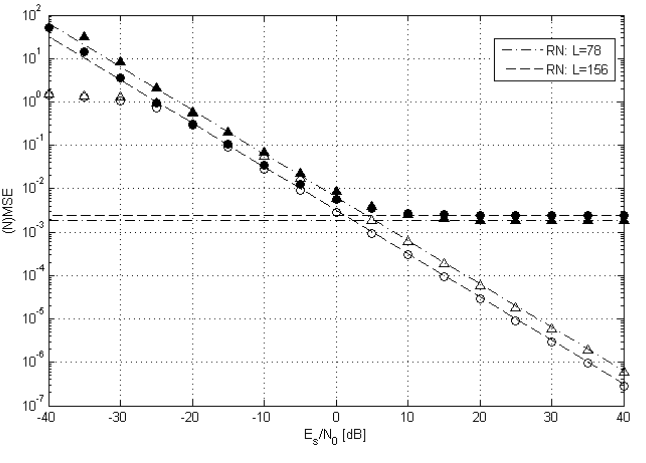

Fig. 6. Estimation accuracy for non-orthogonal codes achieved by correlation

Note also that the angle exhibits *no* jitter floor, a phenomenon not reported in previous publications on this topic so far. It is explained by the fact that all feeds transmit their assigned UW in a *symbol-synchronous* manner. Moreover, each of the sequences travels through the same physical path down to the UT, thus determined by the same attenuation and the same time shift. Taking this into account, it is clear that the correlation process does not affect the phase of the channel estimate so that, in contrast to the amplitude, no jitter floor is present.

It is important to understand that the jitter floor is *not* related to the use of linearly dependent sequences as such. Instead, it is caused by the correlation method, which had to be applied for linearly dependent UWs due to the lack of a pseudo-inverse. For the sake of completeness, Fig. 6 visualizes also the (normalized) MSE for an RN code composed of linearly independent vectors with length $L = 156$ (simulation results for magnitude/phase indicated by solid/open dots). It is also identified that the value of L plays a minor role so as to decrease the floor.

For $E_s/N_0 = 40$ dB and $L = 78$, Fig. 7 shows the top view of the jitter floor as a function of the geographical location. It obviously exhibits larger variations depending on the UTs' positions. By inspection of the plot, it can be seen that the major part of the coverage zone is affected by a value about 10^{-2}, only small areas have a floor lower than 10^{-3}. Although not shown due to limited space, this has been observed with other non-orthogonal codes as well, like Gold or Kasami schemes, as soon as they are applied to a correlation procedure for estimation purposes.

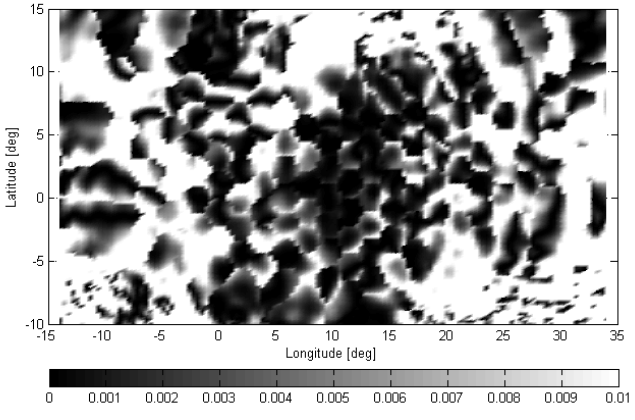

Fig. 7. Top view of estimation accuracy for non-orthogonal codes achieved by correlation ($E_s/N_0 = 40$ dB, $L = 78$)

5 Concluding Remarks

Assuming a multi-beam concept for next generation broadband satellite systems, several algorithms for channel estimation on the forward link have been investigated. By both analytical and simulation results, it could be confirmed that orthogonal training sequences – with Walsh-Hadamard codes as most prominent example in this

respect – are best suited for this purpose. Due to the restricted application of the latter, non-orthogonal sequences were explored in this context. It turned out that a set of linearly independent vectors, which is basically only possible if their length is equal or greater than the number of links (antenna feeds), ends up in a significant degradation of the jitter performance due to an amplification of noise, introduced by the pseudo-inverse of the matrix containing the unique words. On the other hand, applying a correlation procedure to extract the channel estimates from a set of non-orthogonal codes (no matter if they are linearly independent or not), yields a jitter floor, mainly determined by the cross-correlation properties of the selected unique words.

Finally, it is to say that carrier frequency/phase and symbol timing have been assumed as perfectly established for channel estimation on the forward link. This is acceptable for UTs, which form already part of the network; in this case, the data following the unique word will be used for estimation and synchronization of carrier and timing, because they are not very much impaired by interferer noise due to precoding. Nevertheless, if a UT is new to the satellite system, then channel estimates, carrier and timing offsets must be jointly acquired. This resembles very much the situation met on the return link, which is subject of ongoing investigations.

Acknowledgments. The work was supported in part by SatNEx-III (Satellite Network of Experts) launched by the European Space Agency for advanced research in satellite communications (ESA Contract No. RFQ/3-12859/09/NL/CLP).

References

1. Gallinaro, G., et al.: Novel Intra-System Interference Mitigation Techniques & Technologies for Next Generations Broadband Satellite Systems. ESA Final Report, Contract No. 18070/04/NL/US (2008)
2. Angeletti, P., Gallinaro, G., Lisi, M., Vernucci, A.: On-Ground Digital Beamforming Techniques for Satellite Smart Antennas. In: Proc. 19th AIAA, Toulouse, France, pp. 1–8 (2001)
3. Angeletti, P., Alagha, N.: Space/Ground Beamforming Techniques for Emerging Hybrid Satellite Terrestrial Networks. In: Proc. 27th AIAA, Edinburgh, UK, pp. 1–6 (2009)
4. Alvarez-Diaz, M., Courville, N., Mosquera, C., Liva, G., Corazza, G.E.: Nonlinear Interference Mitigation for Broadband Multimedia Satellite Systems. In: Proc. 3rd Int. Workshop Satellite and Space Commun., Salzburg, Austria, pp. 61–65 (2007)
5. Millerioux, J.P., Boucheret, M.L., Bazile, C., Ducasse, A.: Iterative Interference Cancellation and Channel Estimation in Multibeam Satellite Systems. Int. J. Satell. Commun. Network 25, 263–283 (2007)
6. Di Cecca, F., Gallinaro, G.: Ground Beamforming and Interference Cancellation for TDMA Based Reverse-Link Access Schemes. In: Proc. Ka-Band Conf., Cagliari, Italy, pp. 1–8 (2009)
7. Mengali, U., D'Andrea, A.N.: Synchronization Techniques in Digital Receivers. Plenum Press, New York (1997)
8. Corrazza, G.E., et al.: Digisat Techniques Review: Hybrid Space-Ground Processing. ESA Technical Note, Contract No. RFQ/3-12859/09/NL/CLP (2010)

9. Caire, G., Debbah, M., Cottatellucci, L., De Gaudenzi, R., Rinaldo, R., Mueller, R., Gallinaro, G.: Perspectives of Adopting Interference Mitigation Techniques in the Context of Broadband Multimedia Satellite Systems. In: Proc. 23rd AIAA, Rome, Italy, pp. 1–5 (2005)
10. Cottatellucci, L., Debbah, M., Gallinaro, G., Mueller, R., Neri, M., Rinaldo, R.: Interference Mitigation Techniques for Broadband Satellite Systems. In: Proc. 24th AIAA, San Diego, CA, pp. 1–13 (2006)
11. Cioni, S., De Gaudenzi, R., Rinaldo, R.: Channel Estimation and Physical Layer Adaptation Techniques for Satellite Networks Exploiting Adaptive Coding and Modulation. Int. J. Satell. Commun. Network. 26, 157–188 (2008)